

5-ALA-induced porphyrin contents in various brain tumors - Implications regarding imaging device design and their validation

Walter Stummer¹, Sadahiro Kaneko^{1,2}, David Black^{3,4}, Eric Suero Molina¹

¹*Department of Neurosurgery, University Hospital of Münster, Münster, Germany*

²*Department of Neurosurgery, Hokkaido University Graduate School of Medicine, Sapporo, Japan*

³*Carl Zeiss Meditec AG, Oberkochen, Germany*

⁴*University of British Columbia, Canada*

Conflicts of interest: Walter Stummer reports consultant and lecture fees by SBI ALA Pharma, NXDC, Medac and Zeiss Meditec

Disclosure of funding: none.

Corresponding author:

Prof. Dr. med. W. Stummer
Department of Neurosurgery
University Hospital of Münster
Albert-Schweitzer-Campus 1, A1
D-48149 Münster
walter.stummer@ukmuenster.de
Tel. +49 251 83 47472
Fax +49 251 83 47479

Abstract

Introduction

Fluorescence-guidance with 5-Aminolevulinic Acid (5-ALA) has been approved for malignant glioma surgery by the European Medicine Agencies (EMA) in Europe and the Food and Drug Administration (FDA) in the USA. Multiple systems have since been developed for visualizing fluorescing Protoporphyrin IX (PPIX). Employing such systems for fluorescence-guided resections implicitly assumes that qualitative fluorescence detection is equivalent to the established standard tested in a randomized setting and approved by EMA and FDA. This assumption needs to be critically assessed. Goal of this study was to define a threshold of fluorescent tissue discrimination under the BLUE400 filter-system (Carl Zeiss Meditec, Oberkochen, Germany), based on the expressed concentration of PPIX (cPPIX) in tumor tissue.

Methods

Utilizing a hyperspectral imaging system, tumor samples from patients harboring different tumor tissues were analyzed. Absolute values of cPPIX were calculated after calibrating the system with fluorescence phantoms with known cPPIX.

Results

524 samples from 162 patients harboring different tumor types were analyzed. Visual fluorescence under the BLUE400 filter was documented by the attending neurosurgeon. A 0.9 µg/ml threshold of cPPIX could be defined as the minimal concentration required to detect and discriminate visual fluorescence.

Conclusion

The current generation of fluorescence microscopes enables fluorescence discrimination in tumor tissue with a threshold of cPPIX of 0.9 µg/ml, thus defining specificity and sensitivity of this technology as initially tested in a randomized trial. Novel technologies should show similar characteristics in order to be used safely and effectively. If more sensitive, such technologies require further assessments of tumor selectivity.

Introduction

Five-aminolevulinic acid (5-ALA) is the only compound to be approved for fluorescence-guided malignant glioma surgery, in Europe in 2007 and later in the US in 2017. Non-fluorescent and colorless 5-ALA is taken up by brain tumor cells and is converted into fluorescent and photosensitizing porphyrins, predominantly protoporphyrin IX (PPIX) within tumor cells. This property is unique to 5-ALA. Other fluorochromes which have since emerged^{11,15,17,19} are injected intravenously and thus contamination by plasma borne fluorochromes or fluorochromes in edema need to be carefully accounted for^{20,27,28}.

5-ALA induced porphyrins can be made visible with conventional surgical microscopes equipped with appropriate filter systems for excitation and observation light. Because PPIX strongly fluoresces in the visible red range at 635 nm, no camera system, video chain, or image processing technologies are required for seeing fluorescence.

Approval for this method was based on a phase III randomized prospective study²³, among other clinical trials^{5,6,14,22}. In this phase III randomized study patients with suspected malignant gliomas were randomized for surgery with or without 5-ALA. All 17 participating centers of the original study were equipped with identical microscopes by Carl Zeiss Meditec to ensure comparability of hardware, i.e. light sources, light source filters and observation filters²⁴. In order to visualize fluorescence but also to permit background discrimination, filters were selected to allow passage of a part of the reflected blue excitation. The specific combination allows visualization of fluorescence with a certain sensitivity to the human eye and has since been used for all first-generation microscope types, such as models by Leica Microsystems (Wetzlar, Germany), Haag-Streit AG (Koeniz, Switzerland) and Carl Zeiss Meditec (Oberkochen, Germany). However, a number of studies have since demonstrated fluorescence to extend further with infiltrating tumor cells into brain adjacent to tumor, without reaching levels strong enough to be perceived by the human eye when using the dedicated filter system^{25,26,29}. Different technologies have been suggested for increasing sensitivity of the method^{18,30,31,33}. Such methods appear useful for more extensive resections but potentially carry the risk of losing selectivity which might greater, perhaps less specific resection with the worry about ensuing neurological deficits³².

With approval by the FDA in 2017 the development of hardware for fluorescence detection received a new incentive. Exoscope systems are being introduced into the market with potential advantages for surgical ergometry and are being adapted to enable fluorescence detection, i.e. ORBEYE (Olympus, Tokyo, Japan) or Synaptive Modus V (Synaptive Medical, Toronto, Canada)^{4,10}. Other systems include endoscopy¹⁶. The common denominator of such systems is the fact that camera systems and video chains are obligatory, projecting the image onto a screen. Thus, surgeons are no longer seeing the surgical site directly but via video chain.

Some systems, e.g. ORBEYE (Olympus, Tokyo, Japan), further rely on a certain amount of image processing to produce an optimized fluorescence image. A third generation of

microscopes captures fluorescence under white light and injects a fluorescence phantom into the overlay of surgical microscopes, a technology similar to this recently published article².

Employing such systems for fluorescence-guided resections implicitly assumes that qualitative fluorescence detection is equivalent to the established standard tested in a randomized setting and approved by EMA and FDA. This assumption needs to be critically assessed.

In order to fulfill the claim that new systems or technologies have performance characteristics comparable to the traditional filter systems used in presently marketed microscopes with fluorescence options (e.g. BLUE400 - Carl Zeiss Meditec, Leica FL400 - Leica Microsystems), such systems require validation, especially if any form of image processing is involved.

Such validation is crucial. If systems were more sensitive at detecting porphyrin fluorescence more extensive surgery with lower specificity might be performed with potential risks to neurological function. At a minimum, the extent and specificity of more sensitive systems need to be carefully assessed. If systems were less sensitive they would simply not discover tumor.

At present, little information is available regarding the exact levels of PPIX fluorescence which can be detected with the human eye using the established filter systems and conventional microscopes. Some lesion might harbor fluorescence below a threshold that can be discriminated using the conventional fluorescence microscope used for surgery. More knowledge regarding such fluorescence will help defining the characteristics for second generation detection devices with the same or greater sensitivity.

To address these issues, we have now measured PPIX concentrations in tissue samples using spectral unmixing (as previously described⁸) in multiple biopsies from a range of tumors and patients. We aimed hereby to determine the threshold of PPIX concentrations that will result in a tissue being perceived as fluorescent using the standard filter combinations, as used for instance in the Carl Zeiss Meditec BLUE400 option, but also to generate a library of tumors and expected fluorescence levels for future reference, based on a standard dose of 20 mg/kg b.w. 5-ALA.

The tissue thresholds of concentration of PPIX (cPPIX) necessary for perceiving a tissue as fluorescent and thus giving more information to the surgeon should provide a reference for future generations of visualization tools for 5-ALA derived porphyrins regarding the required sensitivity and specificity of detected fluorescence in comparison to the gold standard, visually perceived fluorescence. Neurosurgeons and manufacturers should be aware of the necessity of validation of such devices to ensure comparability to first generation microscopes or to detect relevant changes in their imaging sensitivity and possibly specificity.

Methods

We included patients with various brain tumors, which were surgically treated at our department and were dosed with 5-ALA either according to routine clinical use, in protocols, or in a compassionate use setting. Any off-label use was subject to specific informed consent by patients or legal guardians. IRB approval had previously been obtained for ex vivo fluorescence measurements. No patient-specific data were recorded. Only a unique sample identifier was generated for statistical assessments and for correlation with anonymized histology as soon as this was available.

All patients were administered 5-ALA (Gliolan®, medac, Wedel, Germany) at a dose of 20 mg/kg b.w., dissolved in tap water (50 ml per 1500 mg) 3 to 4 hours prior to induction of anesthesia as previously described²² as part of standard of care. Surgery was performed with an OPMI Pentero (Carl Zeiss Meditec, Germany) equipped with the BLUE400 option.

During surgery, tissues prone for histological assessment were collected and samples immediately placed in vials with light protection and a small amount of ringer's lactate to avoid dehydration. Fluorescence status, as visually assessed using the surgical microscope was recorded by the surgeon. Samples were transported to the laboratory and immediately assessed for PPIX fluorescence using spectrography as previously reported⁸. Immediately after fluorescence analysis, all samples were forwarded for standard neuropathological assessment. Normal brain samples were acquired from epilepsy procedures where temporal lobe resections were indicated. We measured these samples following the same protocol utilized for the tumor biopsies.

Spectrometry

Using a hyperspectral imaging system, spectroscopy was performed in the analyzed tissue as previously described⁸. Via a liquid light guide, a light source (light-emitting diode, LED) was installed in an OPMI PICO (Carl Zeiss Meditec, Oberkochen, Germany), enabling transmission of detected light to a scientific complementary metal-oxide-semiconductor (sCMOS) camera with a high quantum efficiency. High sensitivity for fluorescence detection was therefore assured. Furthermore, a Liquid Crystal Tunable Filter (LCTF) was placed between an achromatic lens and the sCMOS camera. A white light image was recorded with a color camera harboring an IMX 252 sensor (Sony, Tokyo, Japan). This image could be superimposed with the acquired fluorescence imaging. A BLUE 400 observation filter was also installed for optional standard fluorescence imaging. The commercially available software LabVIEW (National Instruments, Inc.; Austin, Tx) was used to control each component of the hyperspectral imaging system. Fluorescence spectra were recorded with the sCMOS camera for the entire wavelength range of the LCTF from 420 to 730nm. Measurements utilizing this imaging system resulted in a fluorescence spectrum and white light spectrum at every pixel, as well as the background signal. The fluorescence spectra were normalized for inhomogeneous scattering and absorption properties across the tissue using the white light spectra. Measurements of fluorescence intensity were performed in 10 regions of interest (ROI) per sample. Reference measurements were performed daily with a non-bleaching reference object (635 nm fluorescence phantom, Carl Zeiss, Oberkochen, Germany).

Calculation of PpIX concentration (cPPIX) was performed with the commercially available software MATLAB (The Math Works, Inc, Natick, MV), as previously described^{9,32}. For this purpose, the system was calibrated using fluorescence phantoms with known cPPIX. PPIX was solubilized in dimethyl sulfoxide (DMSO) at a stock concentration of 10mg/ml. Phantoms were created in different concentrations, focusing on low levels of PPIX (1, 0.75, 0.5, 0.25, 0.125, 0 µg/ml, figure 1) by dilution of the stock with further DMSO. Lipovenoes-20% (Fresenius Kabi, Bad Homburg, Germany), was used to simulate the scattering properties of brain tissue, and yellow food dye (McCormick, London, Canada) was added to provide tissue-like absorption. The dye consists of FD&C yellow 5 and FD&C red 40, and provides absorption in the excitation and emission frequencies of PPIX, while lipovenoes-20% has been shown to be an effective scattering agent in tissue phantoms³. The phantoms were initially mixed to have a range of scattering and absorption coefficients at the excitation and emission wavelengths of PPIX representing the variety present in brain tissue, as described by Valdés et al.³³, but for consistency in the concentration calibration, average values of both coefficients were chosen, with the corresponding concentrations of food dye and lipovenoes-20%. The phantoms were measured using the previously described hyperspectral device, and the generated spectra were unmixed as usual to obtain a magnitude coefficient for the PPIX basis spectrum at each selected region of interest in every phantom measurement. As expected, the PPIX coefficient was linearly related to the known concentration with an r squared value of 0.9986. Thus it was possible to simply scale the PPIX coefficients by the slope of the fitted line to obtain absolute PPIX concentrations (cPPIX). The phantom PPIX coefficients with the fitted line are plotted in figure 2 for low concentration ranges, as is a box plot showing the resultant calculated absolute cPPIX values based on the calibration.

Statistical methods

All statistical analyses were performed with SPSS Statistics 26.0 software (IBM, Armonk, New York, USA) and used for calculating descriptive variables (means, medians, confidence intervals, ranges, maxima and minima). Classification analyses were performed using reporting operating characteristic (ROC) curves and the Youdan's J statistic³⁴ for identifying the best cutoff for cPPIX as a predictor of fluorescence. The J statistic was calculated as

$$J = \text{sensitivity} + \text{specificity} - 1,$$

i.e.

$$J = (TP/(TP + FN)) + (TN/(TN + FP)) - 1$$

where TP is true positives, FN false negatives, TN true negatives and FP false positives.

Youden's J statistics were calculated for every cPPIX value with the fluorescence status used as a classifier ("fluorescence" or "no fluorescence") and plotted over cPPIX to determine the

greatest distance of the ROC curve from the diagonal reference line for identifying the best cutoff.

Differences in cPPIX among samples stratified by tumor type and, if available, fluorescence status, were tested using a one-way analysis of variance with post hoc Tamhane's T2, assuming unequal variances. Boxplots give medians as horizontal bars, 1st and 3rd quartiles as boxes, whiskers as 1.5 x interquartile range, outliers (between 1.5 to 3 x interquartile range) as circles and extreme values (beyond 3 x interquartile range) as "x".

Results

Table 1 provides an overview of patient population (adult and pediatric), tumor types and samples, and patient numbers that provided the basis for this analysis. 524 samples from 162 patients harboring different tumor types were analyzed. Samples are further stratified by visual fluorescence impression as perceived with the Carl Zeiss Meditec BLUE400 option. As expected, significant visible fluorescence was found among various gliomas, but also in meningiomas, in pediatric anaplastic ependymomas, pilocytic astrocytomas and one example of an anaplastic pleomorphic xanthoastrocytoma. Little visible fluorescence was observed in pituitary adenomas and no fluorescence in pediatric medulloblastomas and a single pediatric patient with pilomyxoid astrocytoma. Protoporphyrin IX concentrations appeared related to the visual fluorescence impression. Not always did differences reach statistical significance compared to normal brain tissue using ANOVA and posthoc Tamhane's T2. However, this was frequently due to the small number of samples in a given subtype. All tumor subtypes with visible fluorescence showed minimal PPIX concentrations that were higher than the upper 95% CI limit of cPPIX in normal brain.

Fig. 3A gives a scatter plot of all individual samples stratified by general tumor group. cPPIX values are plotted over autofluorescence at 504 nm, which per se had no relationship to cPPIX but resulted in a greater dispersion of points for clarity. Note the logarithmic scales. The graph demonstrates the heterogeneity of PPIX accumulation in each tumor subtype, its distribution over a wide range and the overlap of fluorescing tumor samples regarding cPPIX. Figure 3B provides the respective box plots of cPPIX stratified by the individual tumor subtypes confirming this assumption. Gliomas and meningiomas are further stratified for those tumor samples with visible and without visible fluorescence. Among samples without visible fluorescence, we were able to identify outliers in some subgroups (low grade and grade III glioma, meningioma, pituitary adenoma) with greater cPPIX concentrations than the majority of samples in these subgroups.

Fig. 4A shows the same samples coded for visual fluorescence impression (none, weak, strong fluorescence), demonstrating overlap regarding cPPIX between samples observed as strongly and those observed as weakly fluorescent. However, samples without visual fluorescence showed only rare instances of overlap with those perceived as fluorescent, indicating a threshold of cPPIX over which samples are perceived as fluorescent. Fig. 4B summarizes the respective boxplots for cPPIX depending on visual fluorescence impression.

In order to test the predictive power of cPPIX as a classifier for visually perceivable fluorescence (as observed with the BLUE400 option), we constructed ROC curves (Fig. 5A). We found the area under the curve to equal .999, 95% CI .998-1.00 p=.000 illustrating a strong power of cPPIX for predicting visual fluorescence and indicating an almost perfect relationship between cPPIX and visible fluorescence. Using Youden's J statistic we next calculated the optimal cPPIX cutoff for discriminating PPIX concentrations, resulting in visible fluorescence from those without visible fluorescence. The optimal cutoff was determined as .895 µg/ml (J statistic: .974, Fig. 5B), resulting in a sensitivity and specificity of both .982. In other words, the Zeiss BLUE400 option allowed visual perception of fluorescence in tissue only if cPPIX was higher than 0.895 µg/ml, with almost perfect discrimination.

Using ROC analysis we also attempted to define the threshold for which the likelihood was highest for perceiving a fluorescent sample as "strongly" as opposed to "weakly" fluorescent when interrogated visually with the BLUE400 option. The AUC was .829 (95% CI: .769 - .889, p= .000, no graph is given) and thus a significant but weaker measure than using cPPIX for predicting any fluorescence. The optimal threshold, as derived from Youden's J statistic, was 9.88 µg/ml (Youden's J: .581, sensitivity .814, specificity .767). In other words, when using the BLUE400 option, if cPPIX exceeded 9.88 µg/ml the surgeon would most likely perceive tissue as strongly fluorescent rather than weakly fluorescent.

Discussion

Validation of fluorescence imaging technologies

With this paper, we objectively measured PPIX concentrations in tissue by spectral unmixing among various tumors of the CNS. We then related this to what surgeon's perceived using a standard first-generation fluorescent microscope (BLUE400, Carl Zeiss Meditec) for visually detecting fluorescence. Using scattergrams and ROC analyses we were able to define a threshold of cPPIX to equal .9 µg/ml to predict visible fluorescence using the particular filters developed for fluorescence-guided resections and tested for efficacy and safety in the pivotal phase III approval study for 5-ALA²³. These analyses also corroborate the fact that fluorescence, when observed under the first-generation microscope, does not appear to be subject to for interpretation or subjective misclassification in light of the sharp threshold found here over a wide range of tumors.

This threshold is further of importance as it closely characterizes the performance of first-generation microscopes with their specific filters for visual discrimination of fluorescence. New generations of imaging technologies for intra-operative fluorescence detection should be tested regarding their discrimination to ensure they are not less sensitive than the eye in conjunction with first generation microscopes, optimally having the same sensitivity, i.e. the same threshold for discriminating 5-ALA-induced porphyrins. If, on the other hand, these methods were more sensitive for detecting and indicating the presence of porphyrins in tumor tissue then they need to be additionally tested carefully for selectivity, i.e. by determining the positive predictive value of fluorescence for identifying tumor.

Novel technical approaches may be grouped according to the underlying technology and degree of image manipulation:

1. alternate filters for visual perception (BLUE400 AR²⁶)
2. video chain with realistic replication of visually perceived fluorescence (Kinevo, Carl Zeiss Meditec)
3. video chain with image processing (ORBEYE, Olympus, Tokyo, Japan)
4. augmented reality systems (Leica Microsystems, Wetzlar, Switzerland²)

Even first-generation filter systems together with high definition video cameras featuring imaging chips with the highest possible resolution and the same color detection as the human eye, in conjunction with a screen system that replicates these colors, still have room for image augmentation. This can be achieved by for instance by increasing video camera shutter times or gain – both factors that might influence fluorescence discrimination. However, as autofluorescence also has a small red component, untoward signal enhancement might result in all tissues showing a red tone. This implies that even video systems requiring testing to ensure true equivalence, for instance when using such systems as the Carl Zeiss Meditec Kinevo, which, when employed as an exoscope, relays fluorescence based on a 4K HD camera.

With the introduction of image processing with the aim of electronically augmenting signals, changing contrasts or color saturation the situation becomes even more complex (e.g. Orbeye). Next generation augmented reality systems with image injection into the visual pathway or the video image allow multiple possibilities for image manipulation. Such devices and their settings should be tested extensively to determine what they are actually showing.

Therefore, we suggest that such devices be subjected to a validation protocol, either in the clinical setting in biological samples or in phantoms. On the other hand, constructing a realistic and reproducible phantom is not without major challenges^{12,26}. Such phantoms should replicate brain and tumor tissue optical properties with specific tissue light absorption and scattering characteristics, autofluorescence, the marked attenuation of light by hemoglobin, which in turn depends on oxygenation and its degree of compartmentalization in red blood cells or vessels and thus the degree of vascularity. Also, the degree of infiltration of tumor cells might play a role and needs to be modeled. Since PPIX is lipophilic, solvents will be required which in turn destroys erythrocytes if such are used to imitate blood in the phantom.

The present analysis does not primarily focus on tumor type, rather on PPIX content in biological specimens collected during fluorescence-guided resections. We have recently published a validation study for a second-generation imaging system with modified filters but still based on visual perception²⁶. In contrast to the present analysis, that validation study was performed on malignant gliomas only, and corroboration of comparability was performed using histology as the gold standard. However, this particular approach is complex and is not without pitfalls. For instance, it relies much on the interpretation of histology by pathologists regarding density and type cells visualized, and will also depend on the types of stains, e.g. immunohistochemistry as opposed to simple H&E. Also, numerous confounders exist such as

the location of biopsies, the number of biopsies per patient and other factors, which are difficult to control and require a detailed and transparent description of procedures²¹. The present analysis via a correlation between perceived fluorescence and cPPIX overcomes the limitations and confounders inherent to histological assessments but still relies on measurements of PPIX in biological specimens.

The results are also pertinent when considering future dosing modi for ALA or the applications of ALA derived fluorescence in brain tumors apart from gliomas.

Histology dependent variations in cPPIX

We observed a wide variation of cPPIX dependent on tumor type and within tumor. While glioblastomas samples uniformly contained high cPPIX, several samples collected from grade III gliomas were without visible fluorescence, while still showing slight elevations of porphyrins. As previously described, a subgroup of low-grade glioma patients had tumors with macroscopic fluorescence which was well in the range of high-grade gliomas, despite histology confirming low grade gliomas and not anaplastic foci. On the other hand, LGG without visible fluorescence displayed a number of samples with slight elevations of cPPIX without these exceeding the cutoff defined above. Similar observations were made for pituitary adenomas. This suggests that more sensitive imaging technologies may be of value for these tumors.

We also used these measurements to readdress the question of “weak” (“pink”, “vague”, “salmon”) and “strong” (“red”, “lava”) fluorescence. This subjective assessment has been related to malignant glioma morphology (solid tumor, infiltrating tumor²⁵) and may be of value when operating malignant gliomas as it allows the surgeon to decide whether he is in non-functional tumor as opposed to approaching functionally intact brain tissue. The present analysis demonstrates a strong relationship between the subjective fluorescence impression and cPPIX, corroborating a high degree of accuracy of human perception at interpreting cPPIX.

Limitations

We provide a unique, large collection of biopsies measured using a continuous hyperspectral system. In this study, we deliver absolute cut-off values of cPPIX and compare them to current standards. It is important to stress that our system was calibrated with fluorescence phantoms in order to deliver an absolute cPPIX based on spectroscopy measurements as previously described^{9,32}. Even though we are certain that the relative values of our measurements are correct, the absolute values depend strongly on the mode of calibration.

While the highly linear nature of our phantoms and effectiveness of the calibration is promising when considering the accuracy of the absolute concentrations, our calibration procedure has certain limitations. The use of food coloring to simulate absorption has been replaced in some studies with bovine blood, and a surfactant is used to avoid PPIX aggregation¹². Furthermore, recent studies have investigated the coexistence of two PPIX photo-states and consequent nonlinearity of PpIX concentration with changing pH and other

microenvironmental differences¹. As the phantoms were all identical except for PPIX concentration, the nonlinear effects are not captured in this calibration. However, as shown by Montcel et al.¹³, the presence of a second photo-state is noticeable only at very low concentrations of PPIX, substantially below the fluorescence visibility threshold obtained in this paper. The effect of this inaccuracy in the phantom calibration on the result of this study should therefore be negligible. Importantly however, the calibration procedure used in this study can easily be reproduced for future reference.

Others have used extractions of PPIX from tumor for determining cPPIX and have found very similar values⁷. These researchers based their calculations on PPIX of various concentration in solutions of tissue dissolved in Solvable (Perkin Elmer LAS, Groningen, The Netherlands) rather than pure solvent we have used. Interactions between PPIX and Soluble cannot be ruled out.

We are currently chemically measuring cPPIX in glioma tissue by extraction to verify and update the calibration of our imaging system. It is therefore possible that after performing these measurements our system will be anew calibrated and absolute values might slightly differ.

Conclusion

We here demonstrate that visualization of fluorescence by first generation fluorescence microscopes with their characteristic filter combinations enable the surgeon to discriminate cPPIX with a sharp threshold of 0.9 µg/ml, thus defining specificity and sensitivity of this technology as initially tested in the randomized trial that led to 5-ALA's approval in malignant glioma surgery²³. Novel technologies should show similar characteristics in order to be used safely and effectively. If more sensitive, such technologies require further assessments of tumor selectivity.

Acknowledgment: Carl Zeiss Meditec for providing us with the hyperspectral imaging system.

Figure Legends:

Figure 1: Measured fluorescence spectra of all phantoms used in the calibration of the hyperspectral measurement device. The intensity values are normalized for absorption and scattering and are thus given in arbitrary units. The calibration focusses on the low concentration range below 1 µg/ml where the threshold of visually perceivable fluorescence was found.

Figure 2: a) Scatter plot of calculated PPIX coefficients using spectral unmixing versus known concentration of the phantom. The orange curve shows a strong linear relation between the PPIX coefficient and concentration, which makes the calibration possible. The calibration factor by which the normalized arbitrary units are multiplied to obtain absolute cPPIX is the inverse of the slope of this line, which is about 11. b) Calculated and calibrated absolute PPIX concentrations vs. known concentration of each phantom. Using the single

calibration factor derived from figure a, this demonstrates accurate mapping between calculated and actual cPPIX.

Figure 3: a) Scatter plot of all individual samples stratified by general tumor group b) respective box plots of cPPIX stratified by the individual tumor subtypes.

Figure 4: a) Tumor samples coded for visual fluorescence impression (none, weak, strong fluorescence), demonstrating overlap regarding cPPIX between samples observed as strongly and those observed as weakly fluorescent and b) Summary of the respective boxplots for cPPIX according to the visual fluorescence impression (boxes with horizontal bars are medians, 1st and 3rd quartiles, whiskers are 1.5 x interquartile range, circle symbols represent outliers (1.5 to 3 x interquartile range) and crosses extremes (> 3 x interquartile range).

Figure 5: a) Receiver operating characteristics curves (ROC) were conducted to assess the predictive power of cPPIX as a classifier for visually perceivable fluorescence. We found the area under the curve to equal 0.999, 95% CI .998-1.00 p=.000, illustrating a strong power of cPPIX for predicting visual fluorescence and indicating an almost perfect relationship between cPPIX and visible fluorescence. b) The optimal cut-off was determined as 0.895 µg/ml (J statistic: 0.974), resulting in a sensitivity and specificity of both 0.982. This means that a cPPIX higher than 0.895 µg/ml in tumor tissue was required in order to visualize fluorescence with the Zeiss BLUE400 filter system.

References

1. Alston L, Rousseau D, Hebert M, Mahieu-Willame L, Montcel B: Nonlinear relation between concentration and fluorescence emission of protoporphyrin IX in calibrated phantoms. **J Biomed Opt** **23**:1-7, 2018
2. Athanasopoulos D, Heimann A, Nakamura M, Kakaletri I, Kempski O, Charalampaki P: Real-Time Overlapping of Indocyanine Green-Video Angiography With White Light Imaging for Vascular Neurosurgery: Technique, Implementation, and Clinical Experience. **Oper Neurosurg (Hagerstown)**, 2020
3. Di Ninni P, Berube-Lauzier Y, Mercatelli L, Sani E, Martelli F: Fat emulsions as diffusive reference standards for tissue simulating phantoms? **Appl Opt** **51**:7176-7182, 2012
4. Doglietto F, Belotti F, Panciani P, Poliani PL, Fontanella MM: High-Definition 3-Dimensional Exoscope for 5-ALA Glioma Surgery: 3-Dimensional Operative Video. **Oper Neurosurg (Hagerstown)** **18**:E82, 2020
5. Feigl GC, Ritz R, Moraes M, Klein J, Ramina K, Gharabaghi A, et al: Resection of malignant brain tumors in eloquent cortical areas: a new multimodal approach combining 5-aminolevulinic acid and intraoperative monitoring. **J Neurosurg** **113**:352-357, 2010
6. Hefti M, von Campe G, Moschopulos M, Siegner A, Looser H, Landolt H: 5-aminolevulinic acid induced protoporphyrin IX fluorescence in high-grade glioma surgery: a one-year experience at a single institution. **Swiss Med Wkly** **138**:180-185, 2008

7. Johansson A, Palte G, Schnell O, Tonn JC, Herms J, Stepp H: 5-Aminolevulinic acid-induced protoporphyrin IX levels in tissue of human malignant brain tumors. **Photochem Photobiol** **86**:1373-1378, 2010
8. Kaneko S, Suero Molina E, Ewelt C, Warneke N, Stummer W: Fluorescence-Based Measurement of Real-Time Kinetics of Protoporphyrin IX After 5-Aminolevulinic Acid Administration in Human In Situ Malignant Gliomas. **Neurosurgery**, 2019
9. Kim A, Khurana M, Moriyama Y, Wilson BC: Quantification of in vivo fluorescence decoupled from the effects of tissue optical properties using fiber-optic spectroscopy measurements. **J Biomed Opt** **15**:067006, 2010
10. Langer DJ, White TG, Schulder M, Boockvar JA, Labib M, Lawton MT: Advances in Intraoperative Optics: A Brief Review of Current Exoscope Platforms. **Oper Neurosurg (Hagerstown)**, 2019
11. Lee JY, Thawani JP, Pierce J, Zeh R, Martinez-Lage M, Chanin M, et al: Intraoperative Near-Infrared Optical Imaging Can Localize Gadolinium-Enhancing Gliomas During Surgery. **Neurosurgery** **79**:856-871, 2016
12. Marois M, Bravo J, Davis SC, Kanick SC: Characterization and standardization of tissue-simulating protoporphyrin IX optical phantoms. **J Biomed Opt** **21**:35003, 2016
13. Montcel B, Mahieu-Williame L, Armoiry X, Meyronet D, Guyotat J: Two-peaked 5-ALA-induced PpIX fluorescence emission spectrum distinguishes glioblastomas from low grade gliomas and infiltrative component of glioblastomas. **Biomed Opt Express** **4**:548-558, 2013
14. Nabavi A, Thurm H, Zountas B, Pietsch T, Lanfermann H, Pichlmeier U, et al: Five-aminolevulinic acid for fluorescence-guided resection of recurrent malignant gliomas: a phase ii study. **Neurosurgery** **65**:1070-1076; discussion 1076-1077, 2009
15. Parrish-Novak J, Byrnes-Blake K, Lalayeva N, Burleson S, Fidel J, Gilmore R, et al: Nonclinical Profile of BLZ-100, a Tumor-Targeting Fluorescent Imaging Agent. **Int J Toxicol** **36**:104-112, 2017
16. Rapp M, Kamp M, Steiger HJ, Sabel M: Endoscopic-assisted visualization of 5-aminolevulinic acid-induced fluorescence in malignant glioma surgery: a technical note. **World Neurosurg** **82**:e277-279, 2014
17. Rey-Dios R, Cohen-Gadol AA: Technical principles and neurosurgical applications of fluorescein fluorescence using a microscope-integrated fluorescence module. **Acta Neurochir (Wien)** **155**:701-706, 2013
18. Sanai N, Polley MY, McDermott MW, Parsa AT, Berger MS: An extent of resection threshold for newly diagnosed glioblastomas. **J Neurosurg** **115**:3-8, 2011
19. Schebesch KM, Proescholdt M, Hohne J, Hohenberger C, Hansen E, Riemschneider MJ, et al: Sodium fluorescein-guided resection under the YELLOW 560 nm surgical microscope filter in malignant brain tumor surgery--a feasibility study. **Acta Neurochir (Wien)** **155**:693-699, 2013
20. Schwake M, Stummer W, Suero Molina EJ, Wolfer J: Simultaneous fluorescein sodium and 5-ALA in fluorescence-guided glioma surgery. **Acta Neurochir (Wien)** **157**:877-879, 2015
21. Stummer W, Koch R, Valle RD, Roberts DW, Sanai N, Kalkanis S, et al: Intraoperative fluorescence diagnosis in the brain: a systematic review and suggestions for future standards on reporting diagnostic accuracy and clinical utility. **Acta Neurochir (Wien)** **161**:2083-2098, 2019
22. Stummer W, Novotny A, Stepp H, Goetz C, Bise K, Reulen HJ: Fluorescence-guided resection of glioblastoma multiforme by using 5-aminolevulinic acid-induced

- porphyrins: a prospective study in 52 consecutive patients. **J Neurosurg** **93**:1003-1013, 2000
- 23. Stummer W, Pichlmeier U, Meinel T, Wiestler OD, Zanella F, Reulen HJ, et al: Fluorescence-guided surgery with 5-aminolevulinic acid for resection of malignant glioma: a randomised controlled multicentre phase III trial. **Lancet Oncol** **7**:392-401, 2006
 - 24. Stummer W, Stepp H, Moller G, Ehrhardt A, Leonhard M, Reulen HJ: Technical principles for protoporphyrin-IX-fluorescence guided microsurgical resection of malignant glioma tissue. **Acta Neurochir (Wien)** **140**:995-1000, 1998
 - 25. Stummer W, Stepp H, Wiestler OD, Pichlmeier U: Randomized, Prospective Double-Blinded Study Comparing 3 Different Doses of 5-Aminolevulinic Acid for Fluorescence-Guided Resections of Malignant Gliomas. **Neurosurgery** **81**:230-239, 2017
 - 26. Suero Molina E, Stogbauer L, Jeibmann A, Warneke N, Stummer W: Validating a new generation filter system for visualizing 5-ALA-induced PpIX fluorescence in malignant glioma surgery: a proof of principle study. **Acta Neurochir (Wien)** **162**:785-793, 2020
 - 27. Suero Molina E, Stummer W: Where and When to Cut? Fluorescein Guidance for Brain Stem and Spinal Cord Tumor Surgery-Technical Note. **Oper Neurosurg (Hagerstown)**, 2017
 - 28. Suero Molina E, Wolfer J, Ewelt C, Ehrhardt A, Brokinkel B, Stummer W: Dual-labeling with 5-aminolevulinic acid and fluorescein for fluorescence-guided resection of high-grade gliomas: technical note. **J Neurosurg** **128**:399-405, 2018
 - 29. Valdes PA, Kim A, Brantsch M, Niu C, Moses ZB, Tosteson TD, et al: delta-aminolevulinic acid-induced protoporphyrin IX concentration correlates with histopathologic markers of malignancy in human gliomas: the need for quantitative fluorescence-guided resection to identify regions of increasing malignancy. **Neuro Oncol** **13**:846-856, 2011
 - 30. Valdes PA, Kim A, Leblond F, Conde OM, Harris BT, Paulsen KD, et al: Combined fluorescence and reflectance spectroscopy for in vivo quantification of cancer biomarkers in low- and high-grade glioma surgery. **J Biomed Opt** **16**:116007, 2011
 - 31. Valdes PA, Leblond F, Jacobs VL, Wilson BC, Paulsen KD, Roberts DW: Quantitative, spectrally-resolved intraoperative fluorescence imaging. **Sci Rep** **2**:798, 2012
 - 32. Valdes PA, Leblond F, Kim A, Harris BT, Wilson BC, Fan X, et al: Quantitative fluorescence in intracranial tumor: implications for ALA-induced PpIX as an intraoperative biomarker. **J Neurosurg** **115**:11-17, 2011
 - 33. Valdes PA, Leblond F, Kim A, Wilson BC, Paulsen KD, Roberts DW: A spectrally constrained dual-band normalization technique for protoporphyrin IX quantification in fluorescence-guided surgery. **Opt Lett** **37**:1817-1819, 2012
 - 34. Youden WJ: Index for rating diagnostic tests. **Cancer** **3**:32-35, 1950

Figure 1. Measured fluorescence spectra of all phantoms used in the calibration of the hyperspectral measurement device. The intensity values are normalized for absorption and scattering and are thus given in arbitrary units. The calibration focusses on the low concentration range below 1 ?g/ml where the threshold of visually perceivable fluorescence was found.

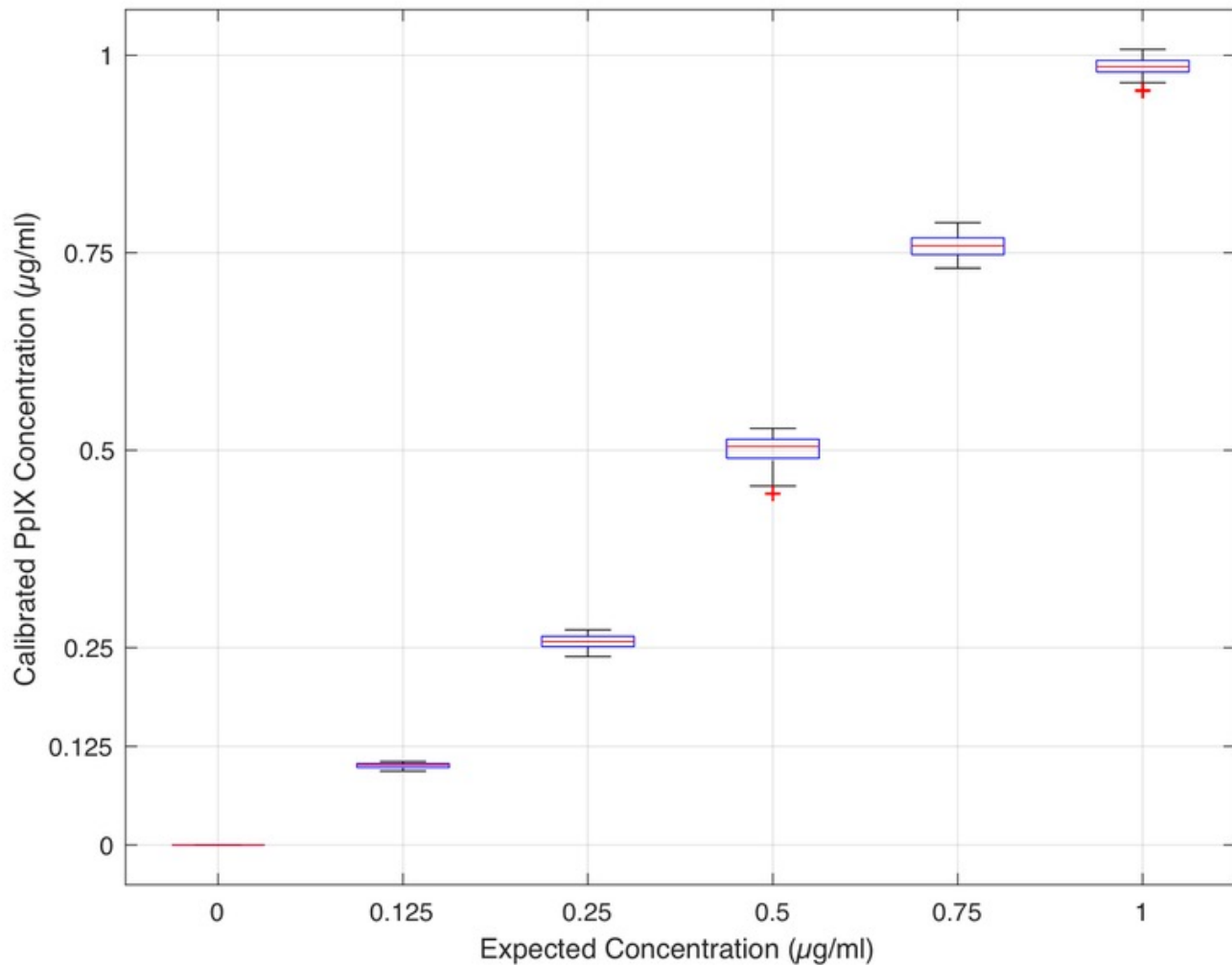


Figure 2a. a) Scatter plot of calculated PPIX coefficients using spectral unmixing versus known concentration of the phantom. The orange curve shows a strong linear relation between the PPIX coefficient and concentration, which makes the calibration possible. The calibration factor by which the normalized arbitrary units are multiplied to obtain absolute cPPIX is the inverse of the slope of this line, which is about 11.

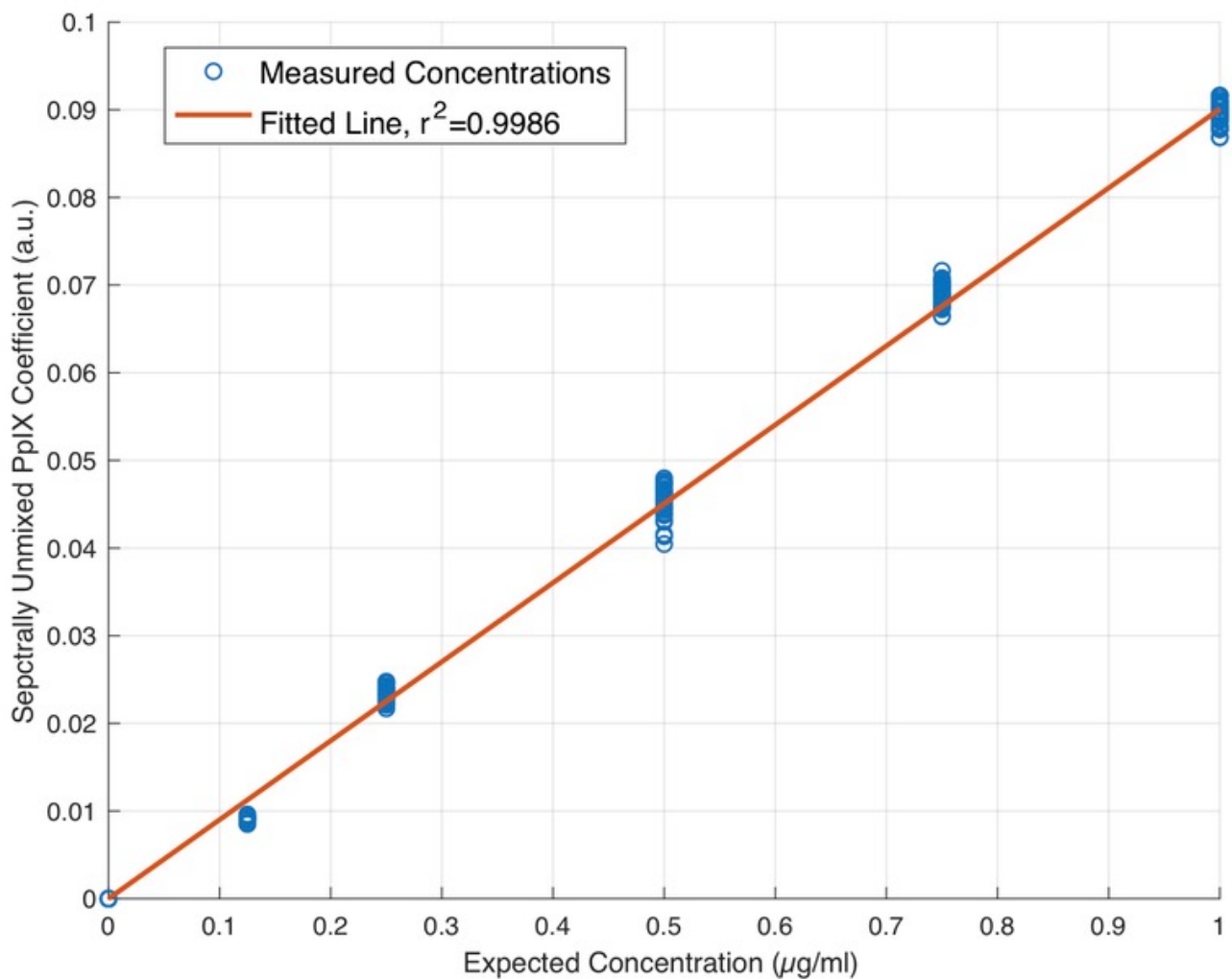


figure 2b. b) Calculated and calibrated absolute PPIX concentrations vs. known concentration of each phantom. Using the single calibration factor derived from figure a, this demonstrates accurate mapping between calculated and actual cPPIX.

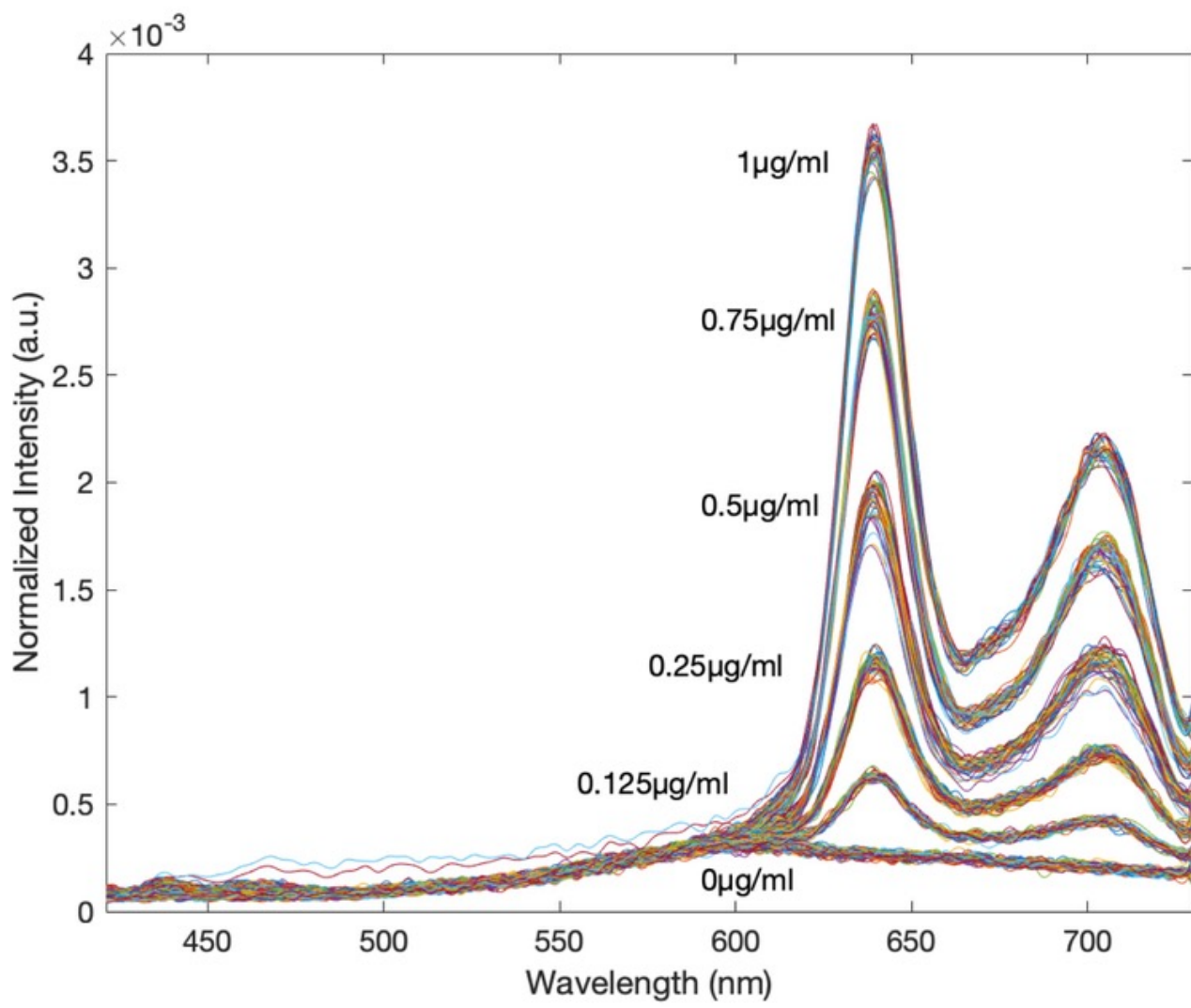


Figure 3a. a) Scatter plot of all individual samples stratified by general tumor group

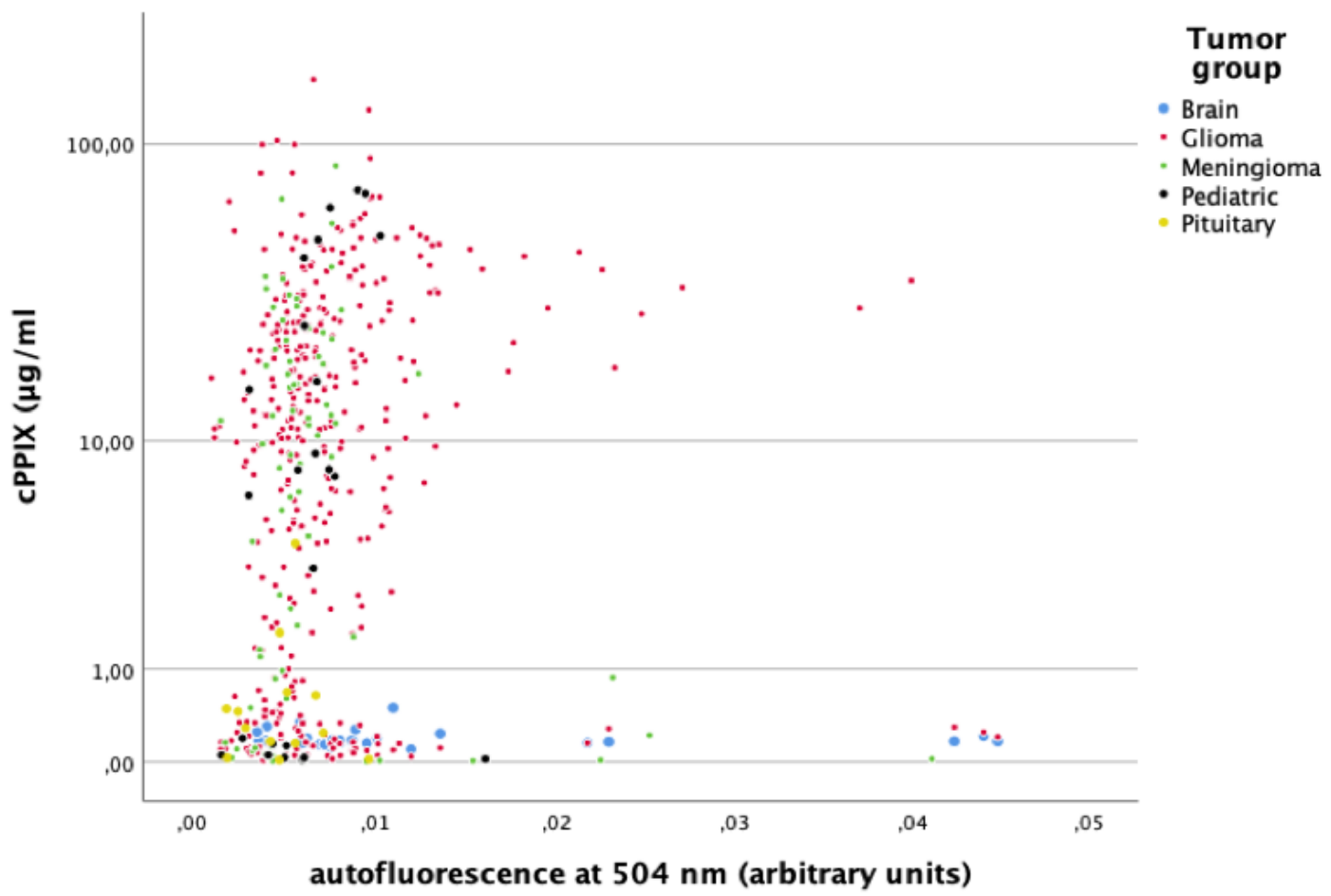


Figure 3b. b) respective box plots of cPPIX stratified by the individual tumor subtypes.

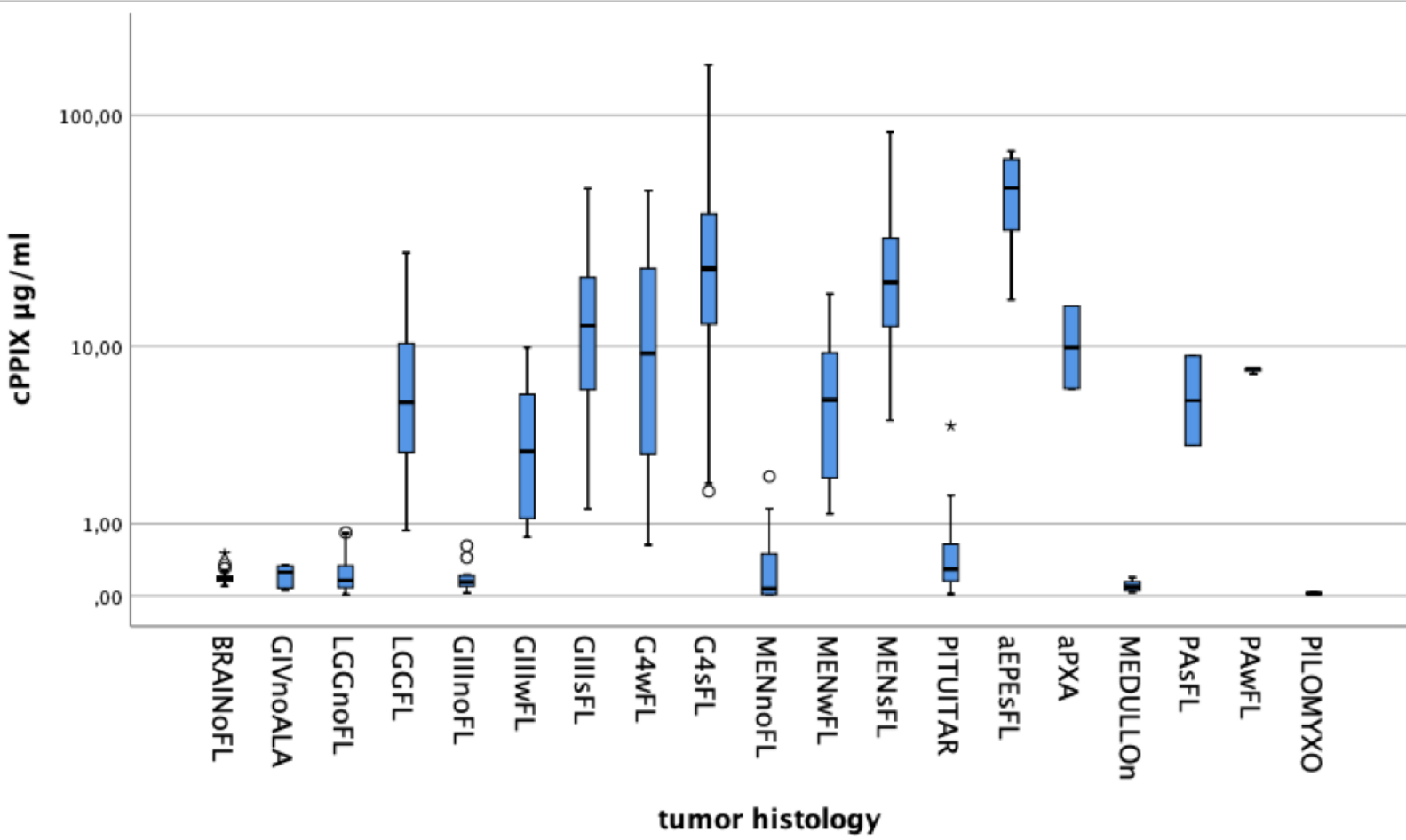


Figure 4a. a) Tumor samples coded for visual fluorescence impression (none, weak, strong fluorescence), demonstrating overlap regarding cPPIX between samples observed as strongly and those observed as weakly fluorescent and

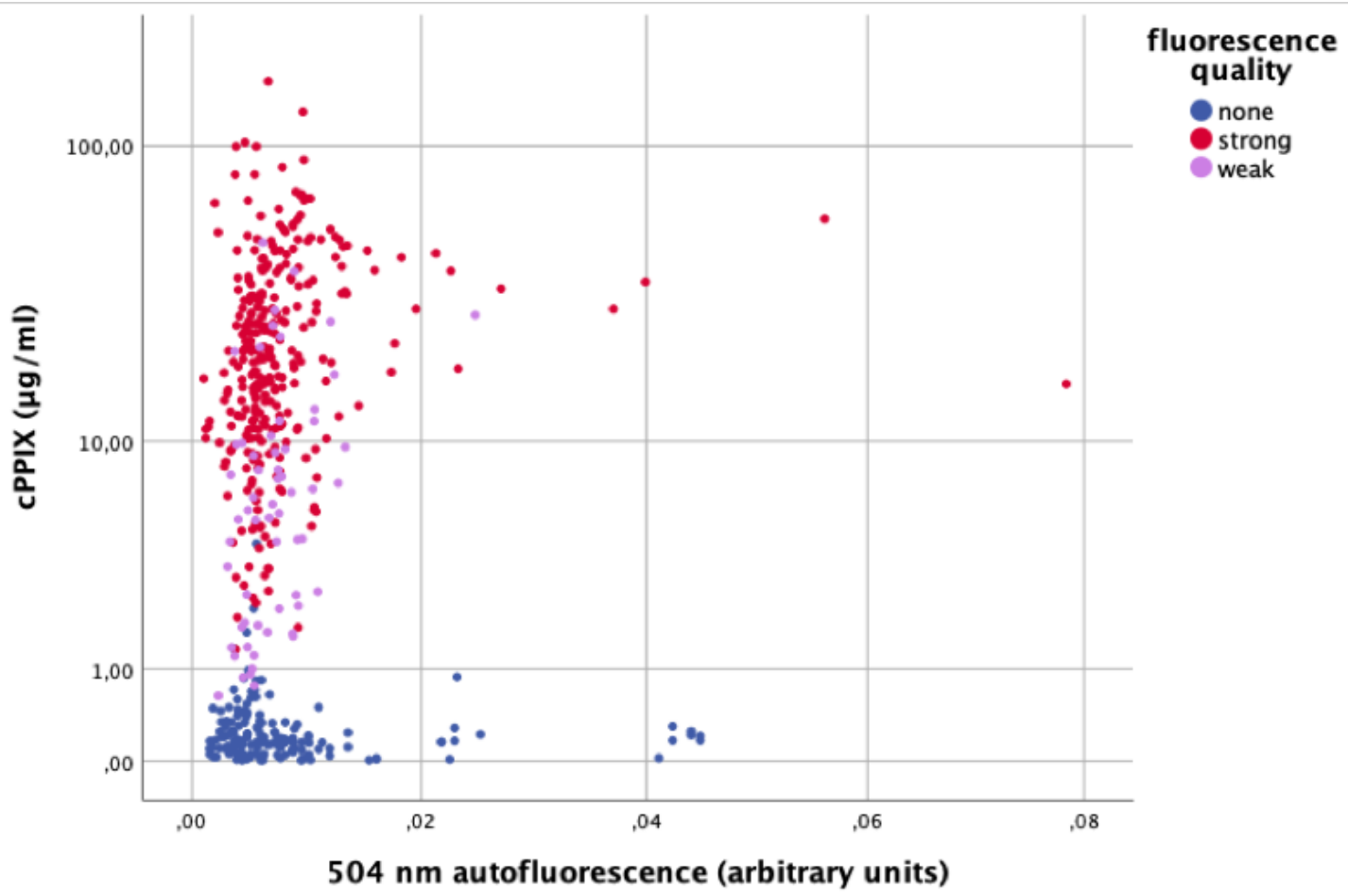


Figure 4b. b) Summary of the respective boxplots for cPPIX according to the visual fluorescence impression (boxes with horizontal bars are medians, 1st and 3rd quartiles, whiskers are 1.5 x interquartile range, circle symbols represent outliers (1.5 to 3 x interquartile range) and crosses extremes (> 3 x interquartile range).

Figure 4b

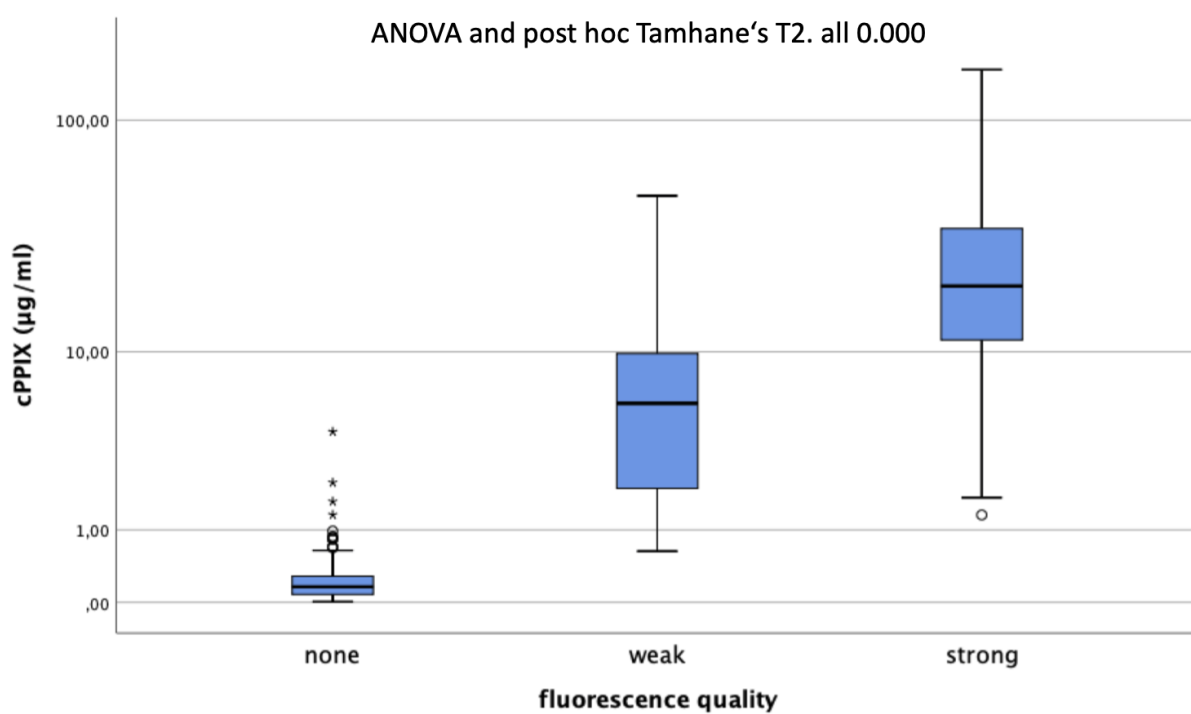


Figure 5a. a) Receiver operating characteristics curves (ROC) were conducted to assess the predictive power of cPPIX as a classifier for visually perceptible fluorescence. We found the area under the curve to equal 0.999, 95% CI .998-1.00 p=.000, illustrating a strong power of cPPIX for predicting visual fluorescence and indicating an almost perfect relationship between cPPIX and visible fluorescence.

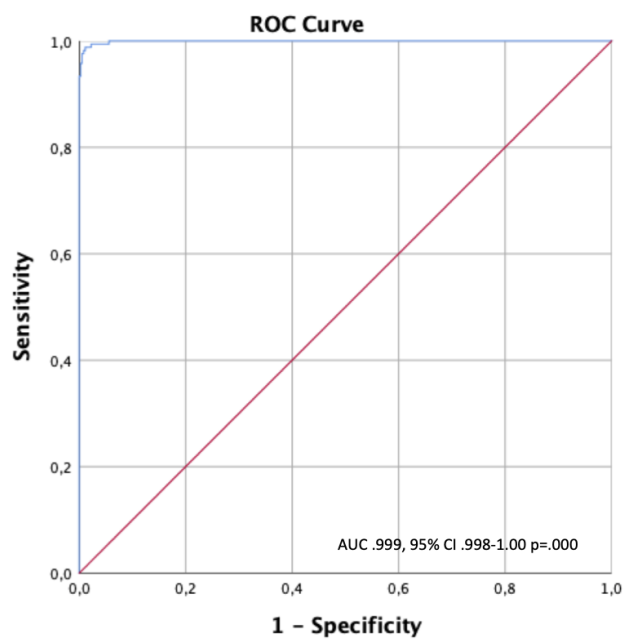


Figure 5b. b) The optimal cut-off was determined as 0.895 ?g/ml (J statistic: 0.974), resulting in a sensitivity and specificity of both 0.982. This means that a cPPIX higher than 0.895 ?g/ml in tumor tissue was required in order to visualize fluorescence with the Zeiss BLUE400 filter system.

